

Your Interlibrary Loan request has been sent by email in a PDF format.

If this PDF arrives with an incorrect OCLC status, please contact lending located below.

Concerning Copyright Restrictions

The copyright law of the United States (Title 17, United States Code) governs the making of photocopies or other reproductions of copyrighted materials. Under certain conditions specified in the law, libraries and archives are authorized to furnish a photocopy or other reproduction. One of these specified conditions is that the photocopy or reproduction is not to be "used for any purpose other than private study, scholarship, or research". If a user makes a request for, or later uses, a photocopy or reproduction for purpose in excess of "fair use", that user may be liable for copyright infringement. This institution reserves the right to refuse to accept a copying order if, in its judgment, fulfillment of the order would involve violation of copyright law.

Interlibrary Loan Services: We Search the World for You...and Deliver!

Interlibrary Loan Services
The Florida State University
711 West Madison Street
Tallahassee, Florida 32306-1005

Lending the FSU Collection: 850.644.4171
James Elliott- ILL- lend@reserves.lib.fsu.edu

Borrowing for the FSU Community: 850.644.4466
Alicia Brown- ill@reserves.lib.fsu.edu

Odyssey: 128.186.59.120 Ariel: 146.201.65.22
Fax: 850.644.3329

MICHIGAN STATE
UNIVERSITY

The Michigan State University Libraries are pleased to supply this material to you from our collection. The MSU library does not hold copyright of this material and cannot authorize any further reproduction.



Interlibrary
Services

MSU LIBRARIES

The copyright law of the United States (Title 17, United States Code) governs the making of photocopies or other reproductions of copyrighted materials. Under certain conditions specified in the law, libraries and archives are authorized to furnish a photocopy or other reproduction. One of these specified conditions is that the photocopy or reproduction is not to be "used for any purpose other than private study, scholarship, or research". If a user makes a request for, or later uses, a photocopy or reproduction for purposes in excess of "fair use", that user may be liable for copyright infringement.

If you have questions, please contact your library.

Michigan State University ILL (EEM)



ILLiad TN: 1169962

ILL Number: -14638064



RAPID

Borrower: RAPID:FDA

Rec Date: 4/22/2019 6:00:45 AM

Lending String:

Call #: PSS

Patron:

Location: MSU ONLINE RESOURCE (01

01, 1991)-

ISSN: 1936-2684

Journal Title: Atomization and sprays 1044-5110

Volume: 16 Issue: 3

Charge

Month/Year: 2006

Maxcost:

Pages: 299-318

Article Author:

Shipping Address:

Article Title: EFFECTS OF INLET SURFACE
ROUGHNESS, TEXTURE, AND NOZZLE
MATERIAL ON CAVITATION

NEW: Main Library

Imprint:

Fax:

Notes:

Ariel: 146.201.65.22

Odyssey: fsu.illiad.oclc.org

Scan in ILLiad

Maybole all

EFFECTS OF INLET SURFACE ROUGHNESS, TEXTURE, AND NOZZLE MATERIAL ON CAVITATION

Jy-Cheng Chang, Shou-Ben Huang, and Chih-Ming Lin*

Department of Mechanical Engineering, Chung Cheng Institute of Technology,
National Defense University, Tamsui, Taoyuan, Taiwan 335, Republic of China

Original Manuscript Submitted: 5/12/03; Final Draft Received: 11/29/04

The aim of this study is to experimentally investigate the effect of inlet surface roughness, texture, and nozzle material on internal flow. Study results show that inlet surface roughness can affect the occurrence of cavitation much more than it affects hydraulic flip. Also, dimensionless driving pressures ranging from 1.28 to 1.48, correspond to the occurrence of cavitation, and ranges of 1.48 to 1.97, correspond to the occurrence of hydraulic flip in an acrylic nozzle. The variation of dimensionless driving pressures corresponding to the occurrence of cavitation caused by changing surface roughness is much greater than that of hydraulic flip, unless the roughness/hole diameter ratio rises to 0.0047. In an acrylic nozzle with a roughness/hole diameter ratio of 0.0115, the phenomenon of hydraulic flip becomes negligible. Increasing the diameter of the nozzle hole can reduce the effect of roughness on cavitation and the occurrence of hydraulic flip. The more adhesion between the wall of the nozzle and water molecules, the less likely is the occurrence of hydraulic flip, and there is a critical value of the dimensionless of the contact angle for the occurrence of hydraulic flip between 1.19 and 1.24 when the ratio of the roughness-to-hole diameter is ~ 0.005. Burrs on the inside wall of the nozzle will eliminate hydraulic flip, even though cavitation exists within the nozzle. Cavitation is not only affected by coupling the ratio of the roughness-to-hole diameter and competition for the contractive and adhesive forces represented, it can also be affected by the surface texture of the nozzle, such as the occurrence of burrs.

INTRODUCTION

It is well known that the fuel injection system of an engine is of primary importance in increasing combustion efficiency and reducing environmental pollution. It is also recognized that the spray structure and penetration, which control the degree of mixing with the air inside the combustion chamber, are determined by the geometry of the nozzle and injection conditions. Bergwerk [1] resolved flow structures inside atomizing orifices by using transparent circular orifices; he concluded that the discharge coefficient was only a function of Reynolds number before cavitation began and was dominated by the cavitation number once the orifice entered the cavitation regime. Bergwerk also reported that asymmetries in the upstream flow passage leading to the orifice and minute irregularities of the inlet corner play critical roles in the cavitation. Hiroyasu et al. [2] and related studies [3, 4] conducted experiments to determine the effect of orifice cavitation on spray properties and concluded that the strong turbulence in the nozzle hole due to the cavitation phenomena contributes greatly to the disintegration of the liquid jet.

*Corresponding author; e-mail: changjc@ccit.edu.tw. This work was supported financially by the National Science Council, ROC, under Contract No. NSC 89-2612-E-014-007. Wei-Chun Wang carried out additional experiments with roughness and made photographs during the revision of the article.

Soterious et al. [5] studied the effects of cavitation and hydraulic flip on atomization of direct-injection (DI) diesel sprays. Chaves et al. [6] reported on cavitation in the nozzle hole of diesel injectors using transparent nozzles; they showed that the length of the cavitation film is not steady, in spite of the steady upstream condition. Henry and Collicott [7] explored the fluid dynamic flow structures in a transparent slot orifice and produced empirical data for comparison to the predictions of Chen and Heister's cavitation model [8]. They concluded that cavitation can be present in orifices as small as 120 μm , at driving pressures as low as 1.5 atm, and that cavitation at inception consists of minute bubbles, which rapidly recondense into the liquid. The structures in cavitation for similar gap size and pressures differ for orifices with different lengths.

Henry and Collicott also concluded that cavitation is very prevalent and dynamic within relatively low-pressure atomizing orifice flows, and it occurs even in the presence of substantial bluntness at the inlet. It should be mentioned that in Hiroyasu's experiments [4], no cavitation and no constricted flow were produced for the nozzle, which had a quadrant sharp at its entrance, even with considerably high injection pressure, up to 200 MPa. The previous review of the literature shows that although there have been some discussions on the generation of cavitation in minute internal flows, there still remain areas where more research is needed. These include the effects of roughness or sharpness on the inlet corner of the nozzle hole. According to Lefebvre [9], if the static pressure in flow regions is lower than the vapor pressure, gas or vapor may be released from the liquid to form bubbles, causing cavitation, which can have a pronounced influence on the discharge coefficient. The subsequent explosion or collapse of these bubbles can also accelerate jet breakup. The normal working range of diesel nozzles is such that both cavitating and noncavitating flow may occur under certain conditions. Nurick [10] investigated the effects of cavitation on spray mixing in circular and rectangular orifices; he presented a model of orifice cavitation and predicted mass flow successfully using his model. Nurick also suggested that cavitation occurs in sharp-edged orifices, leading either to hydraulic flip or reattachment.

Recent studies [11, 12] suggest that if the corner of the inlet is sufficiently sharp, the flow tends to separate and form a *vena contracta* inside the nozzle. The contraction in the inlet effectively reduces the area of the liquid flow. This reduced area is accompanied by increasing velocity, predicted by conservation of mass. The conservation of mass predicts that the acceleration of the liquid through the *vena contracta* causes a pressure depression in the throat of the nozzle. Low pressure inside the throat of the nozzle may fall below the vapor pressure of the liquid, causing cavitation. Koivula [13] also reported that, because of increased velocity of flow in *vena contracta*, the dynamic pressure head is increased, thereby decreasing static pressure. When static pressure in *vena contracta* is decreased to the evaporation pressure of a liquid, cavitation occurs. Cavities traveling along the flow collapse when they enter the high-pressure region of flow. The studies mentioned above, however, do not concentrate on quantifying the sharpness of the nozzle inlet corner. The authors attempt to indirectly quantify sharpness of the nozzle inlet corner by grinding the surface of the nozzle inlet to create different surface roughness, or texture. This paper attempts to perform a more comprehensive investigation on this topic. To obtain detailed information about the generation of cavitation in the internal nozzle flow, a simple hole nozzle was made and incorporated into a steady-flow rig. In the next section, the experimental system is described, followed by discussion of the results and conclusions.

EXPERIMENTAL SYSTEM

Figure 1 shows the schematic diagram of the injection equipment. Water at room temperature, 20°C, was pressurized by N₂ gas in an accumulator and supplied to the nozzle. The differential pressure of the injection was adjusted by a needle valve and measured by a Bourdon tube pressure gauge and a pressure transducer whose signal was sent to an A/D converter, built into a personal computer. The water was injected from the nozzle into the atmospheric air. The photography and image capture system used in this project was assembled from a MLH-10 macroscopic lens made by Computar, together with a CCD camera made by SAKAI, an HR-S2100T video recorder made by JVC, an image capture card made by Matrox, a personal computer, and a 1531 stroboscope, made by the General Radio Company. The stroboscope was used to produce a 1.2 µs pulse of light emitting onto the nozzle or the jet, which image was observed by the CCD camera positioned at the axis of illumination. The illumination axis lay in the cross-stream direction. The water flow rate through the injection nozzle was measured at various differential pressures of injection using the flow meter, or by sampling the injected water in a graduated cup.

Figure 2 shows the schematic drawing of the injector. The typical nozzle had a single hole, 0.7 mm in diameter and made of transparent material; its length was set to 1.4 mm (length-to-diameter ratio L/D = 2). The upstream chamber of the nozzle hole was 6.5 mm in diameter and 127 mm in length. These nozzle sizes were chosen in the same dimensions as used by Nishida et al. [14] and Tamaki et al. [3], for the purpose of comparison to their work. To compare the sharpness of the inlet hole for different nozzles and to verify their affect on internal flow, photos of the inlet holes were taken before assembling the nozzle, using microphotography.

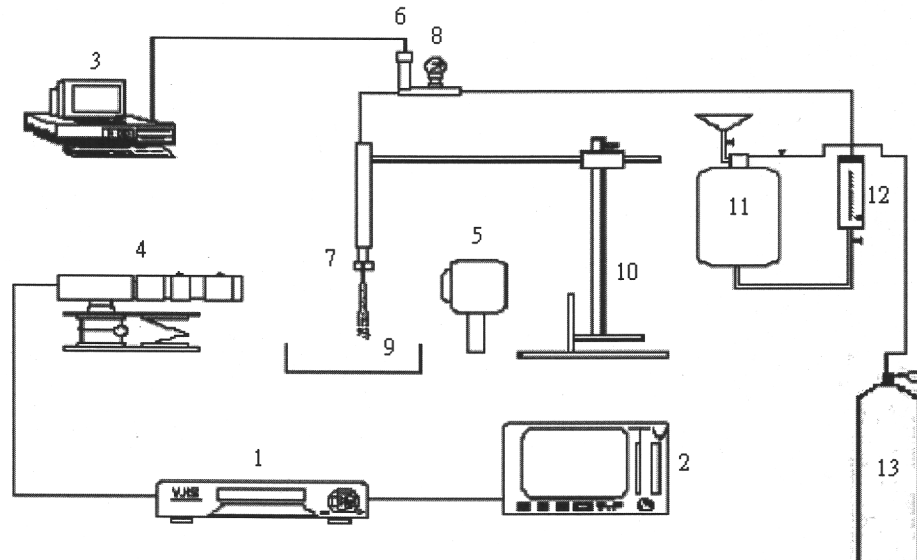


Fig. 1 Schematic diagram of the injection equipment: 1. Video recorder; 2. monitor; 3. personal computer; 4. macroscopic-lens and CCD camera; 5. stroboscope; 6. pressure transducer; 7. nozzle; 8. pressure gauge; 9. collector; 10. 3-D traversing; 11. accumulator; 12. flow meter; 13. N₂ gas.

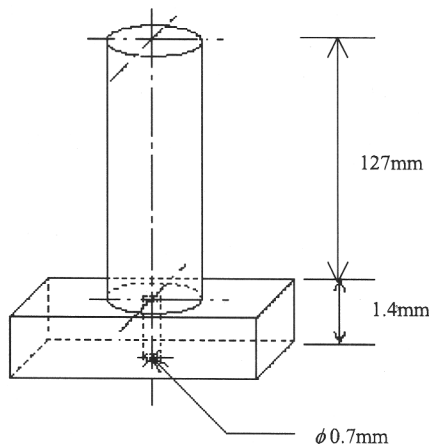


Fig. 2 Schematic drawing of the injector.

RESULTS AND DISCUSSIONS

As previously mentioned, if the static pressure in the flow regions is lower than the vapor pressure, gas or vapor may be released from the liquid to form bubbles and cause cavitation. According to Gerhart et al. [15] and Sears et al. [16], surface tension, or surface energy, describes the forces that interface a gas and a liquid (e.g., water-air), two liquids, or one or more liquids, a gas, and a solid (e.g., water-air-glass). The relative magnitudes of the surface energies determine the shape of liquid surfaces that are in contact with solids and other fluids (usually air). For the specific liquid-solid combinations, which are classified as wetting or nonwetting, surface tension can be related by the value of the contact angle between the liquid and solid surfaces using Young's law [17]. It should be mentioned again that surface films will exist not only between a liquid and a gas, but between a solid wall and a liquid, and a solid and a vapor, whenever cavitation occurs in the nozzle hole. For example, the curvature of the surface of a liquid near a solid wall depends on the difference between the surface tension of the solid-vapor film (χ_{SV}), and the surface tension of the solid-liquid film (χ_{SL}). Because the values of χ_{SL} and χ_{SV} are not readily available, Young's equation [17] can be used to relate their difference, $\chi_{SV} - \chi_{SL}$, to χ_{LV} (the surface tension of the liquid-vapor film), and the contact angle θ :

$$\chi_{LV}\cos\theta = \chi_{SV} - \chi_{SL}$$

In order to investigate the effect of surface tension on the cavitation [i.e., the effect of competition for the attractive force between water-to-water ("contractive force" [18]), and water-to-nozzle material molecules ("adhesive force" [18]), on the cavitation], the contact angle is used and can be measured, since it is uniquely related to the surface tension. Also, the surface tension of the liquid-vapor film can be obtained from the *Handbook of Chemistry and Physics* [19]. For simplification and systematization, only water was used as the working fluid, and the temperature was kept at 20°C for fixing the value of the vapor pressure. Since vapor pressure is a function of liquid and temperature, five materials were used as the nozzle material for varying the surface energy (or the tension of the liquid-vapor

film). First, the acrylic was used as the nozzle material in the experimental since the internal flow can be seen clearly. The effect of the roughness of the nozzle inlet surface on cavitation will be described and discussed first, followed by the results of the effect of the surface tension on the cavitation.

EFFECT OF ROUGHNESS OF NOZZLE INLET SURFACE ON CAVITATION

An acrylic nozzle with $L/D = 2$ and diameter D of 0.7 mm was fabricated, while its inlet surface was not—or was ground using a different grit-numbered sandpaper—before being connected to the upper stream chamber. This resulted in different roughnesses, corresponding to the serial grit numbers of 1000, 800, 400, 240, 180, and 40. Figure 3 shows the top view images of the nozzle hole. The behavior of the liquid flow in the nozzle and the liquid jet near the exit of the nozzle is shown in Fig. 4, where the flow is directed downward; the upper part of the image is the nozzle, and the lower part is the jet.

Comparing the driving pressure of cavitation occurring in the nozzle in Fig. 4 shows that varying the roughness by grinding the nozzle inlet surface with grit-numbered sandpaper from 1000 to 180, affects the driving pressure very little at the onset of cavitation. Also, when hydraulic flip takes place (cavitation has fully developed and the liquid has totally left the inner wall of the nozzle, so that the diameter of the existing liquid jet is less than the nozzle hole diameter), the surface of the jet exhibits more disturbances using the rougher inlet surface. Table 1 lists injecting pressures (dimensionless) when cavitation or hydraulic flip occurs in the nozzle using different inlet surface roughness created by grinding with different grit-numbered sandpapers. The symbol V indicates the occurrence of cavitation and O indicates hydraulic flip. In the table it can be seen that inlet surface roughness can affect the occurrence of cavitation much more than that of hydraulic flip. Moreover, the dimensionless driving pressure ranges from 1.28 to 1.48, depending on the occurrence of cavitation, and 1.48 to 1.97, corresponding to the occurrence of hydraulic flip for the acrylic nozzle and variation of the dimensionless driving pressure, which

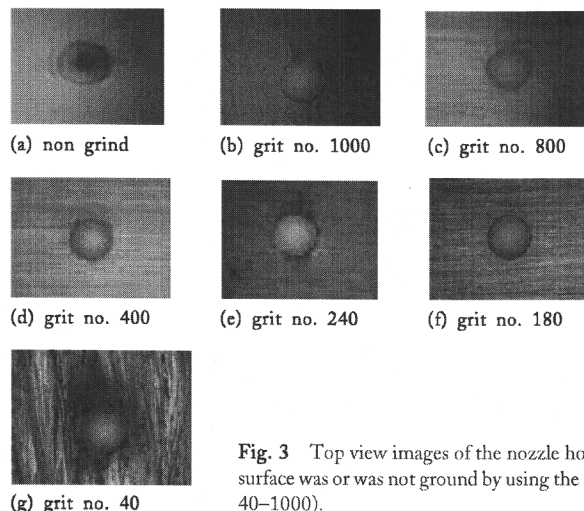


Fig. 3 Top view images of the nozzle hole with $L/D = 2$ and $D = 0.7$ mm; the inlet surface was or was not ground by using the different grit number of sandpaper (grit no. 40–1000).

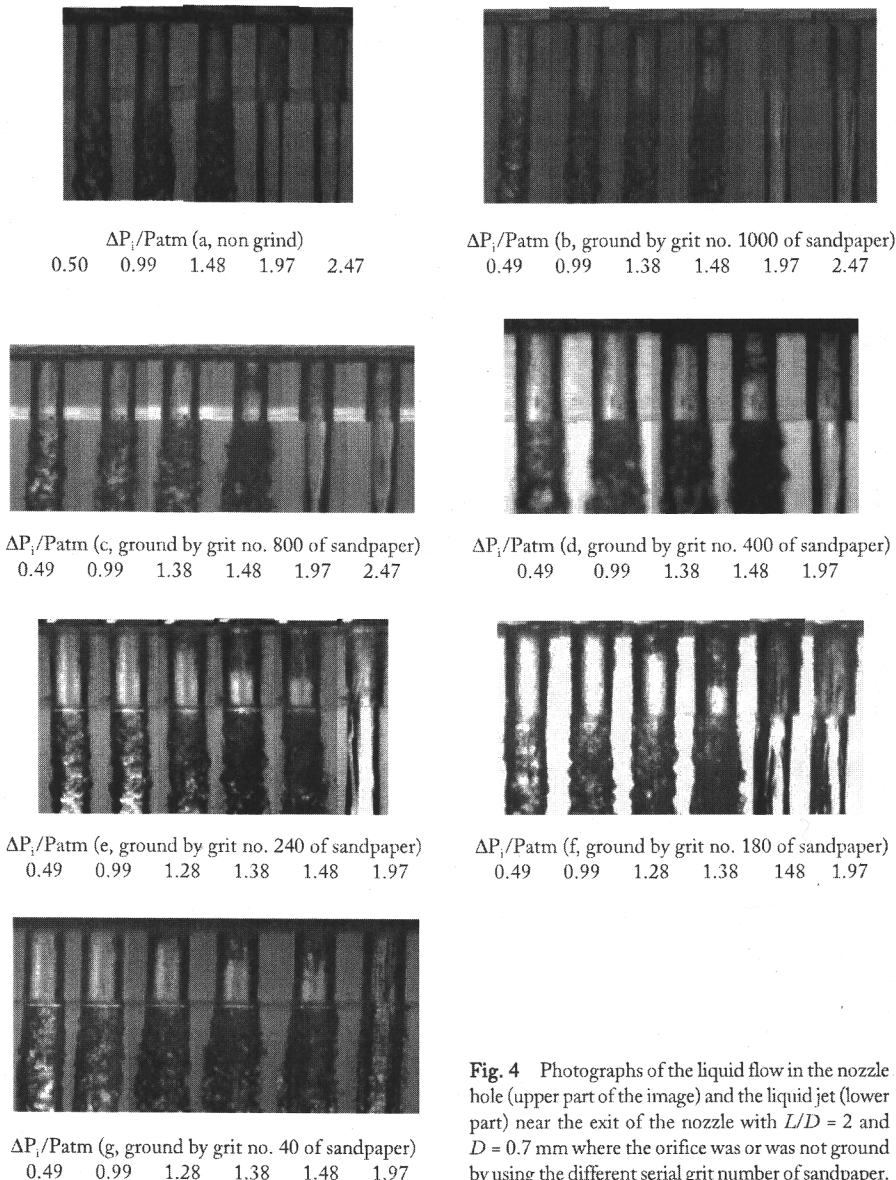


Fig. 4 Photographs of the liquid flow in the nozzle hole (upper part of the image) and the liquid jet (lower part) near the exit of the nozzle with $L/D = 2$ and $D = 0.7$ mm where the orifice was or was not ground by using the different serial grit number of sandpaper.

corresponds to the occurrence of cavitation, because changing surface roughness has a much greater effect than hydraulic flip, except when using a 180 grit-numbered sandpaper, which results in roughness of $3.29 \mu\text{m}$ (shown in Table 2). More details about this table will be described later. It is interesting to note that when the inlet surface is ground with number 40 grit paper, resulting in roughness of $8.05 \mu\text{m}$ (shown in Table 2), the phenomenon of hydraulic flip is not obvious since the existing jet exhibits much turbulence on the surface and some liquid drops disintegrate from the jet. Overall, the above results

Table 1 Injecting Pressure (Dimensionless) When Cavitation or Hydraulic Flip Occurs in the Nozzle with Different Inlet Surface Roughness Created by Grinding for Using Different Grit Number of Sandpaper

		$\Delta P_i /P_{atm}$						
Grit no.	of Sandpaper	0.49	0.99	1.28	1.38	1.48	1.97	2.47
Non grind					V	O		
1000				V		O		
800					V	O		
400				V		O		
240			V			O		
180			V			O		
40		V						

Note: $P_{atm} = 0.101325 \text{ MPa}$; V: indicates cavitation onset; O: indicates hydraulic flip onset.

indicate that the roughness of the nozzle inlet surface has some effect on the occurrence of hydraulic flip and cavitation.

It should be mentioned that the roughness of the nozzle inlet surface has direction (or orientation) (as shown in Fig. 3), because of the orientation of the grinding path. Figure 5 shows a schematic drawing of the different direction (or orientation) of the camera shot. The roughness of the surface is measured in a way that shows the statistical average behavior of the surface height, R_a . Figure 6 is a schematic drawing of the moving direction of the stylus, corresponding to the direction of the sandpaper's grinding. Three kinds of surface roughness are measured in the experiment: first, the surface roughness is measured when the stylus' moving direction is set to the same orientation as the sandpaper grinding. The second measurement is in the direction perpendicular to the orientation of the sandpaper grinding, and the third measurement is the surface roughness when the nozzle inlet surface is ground without orientation. Table 2 lists the measured roughness of the inlet surface of the nozzle corresponding to Fig. 5.

Figures 7 and 8 show different side images of the nozzle. The photographs show that when the grinding direction is perpendicular to the camera shot, the cavitation bubble

Table 2 Roughness of the Inlet Surface in the Acryl Nozzle with $L/D = 2$ ($D = 0.7 \text{ mm}$). The Nozzle Was or Was Not Ground by Different Serial Grit Number of Sandpaper

Grit no. of sandpaper	Roughness of nozzle inlet surface after grinding R_a (direction of grinding relative to direction of camera shot), unit: μm	
	Perpendicular	Parallel
Non grind	0.0372	0.0372
1000	0.4785	0.4304
800	1.0090	0.5788
400	1.1420	0.6268
240	2.7630	0.9617
180	3.2910	0.9842
40	8.0520	1.5710

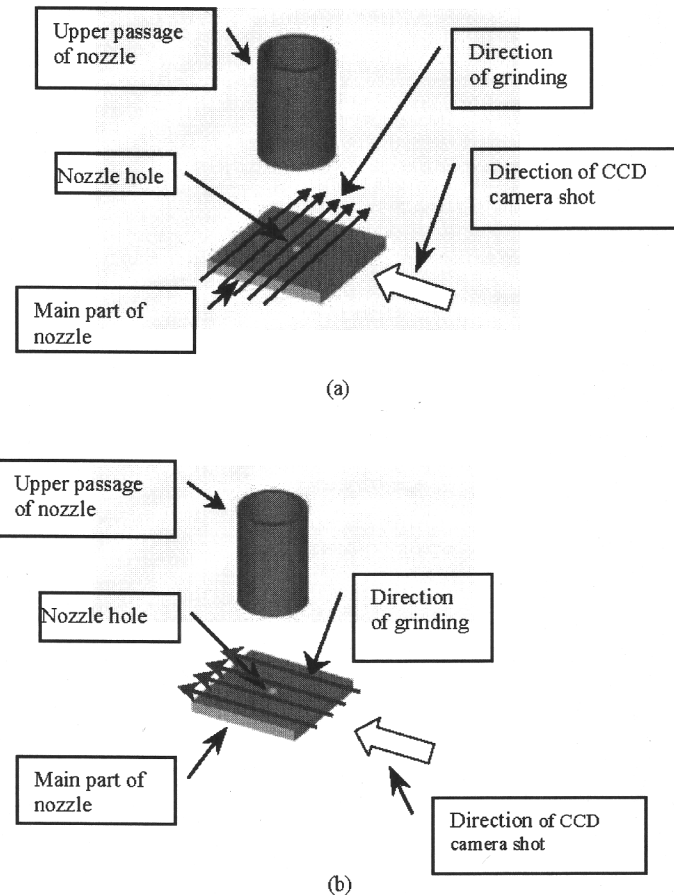


Fig. 5 Schematic drawing of the different direction of CCD camera shot: (a) perpendicular (front view); (b) parallel (side view).

almost begins to occur at both sides of the nozzle hole image (as shown in Fig. 7b). However, when the direction of grinding is parallel to the direction of the camera shot, the cavitation bubble almost begins to occur at the *center* of the nozzle hole image (as shown in Fig. 8b). It is interesting to note that the shape of the exiting liquid jet can also be affected by the roughness direction of the nozzle's inlet surface, as shown in Fig. 9, where the shape of the jet is flat instead of circular. It is worthwhile investigating the inlet surface of the nozzle more closely to determine why the direction (or orientation) of grinding affects the first position of cavitation that occurs. Figure 10 shows the amplified images of the inlet surface of the nozzle hole with $L/D = 2$ ($D = 0.7$ mm), where the center image is magnified by 100 times, others images are magnified 200 times, and the orifice was ground with grit number 40 sandpaper. The images show that the surfaces at the upper and lower areas near the inlet of the nozzle look rougher than surfaces at the right and left sides of the nozzle. It is also notable that the directional grinding results in obviously uneven surface texture around the nozzle hole, but with directional roughness at the nozzle inlet surface, increasing

the roughness measurement to $8.05 \mu\text{m}$ when the stylus moves perpendicular to the grinding direction and to $1.57 \mu\text{m}$ roughness when the stylus moves in the same orientation as the grinding direction. The above fact implies that the directional roughness at the nozzle inlet surface can affect the occurrence of hydraulic flip and the shape of the injecting liquid jet.

To further clarify the effect of roughness on cavitation and hydraulic flip occurrence, two more nozzles ($L/D = 2$, $D = 1 \text{ mm}$ and 1.5 mm) were fabricated (see Fig. 11). Figure 12 shows photographs of liquid flow in a nozzle hole with $D = 1 \text{ mm}$. It is interesting to note that the distribution of the cavitation bubbles is even. Similarly, the distribution of the

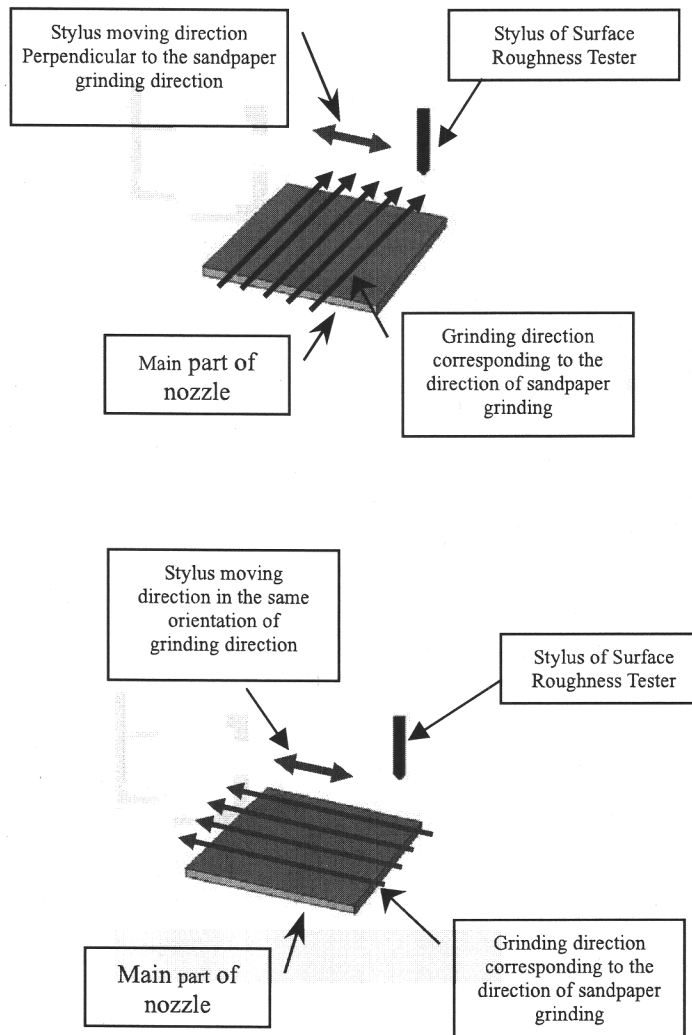


Fig. 6 Schematic drawing of stylus moving.

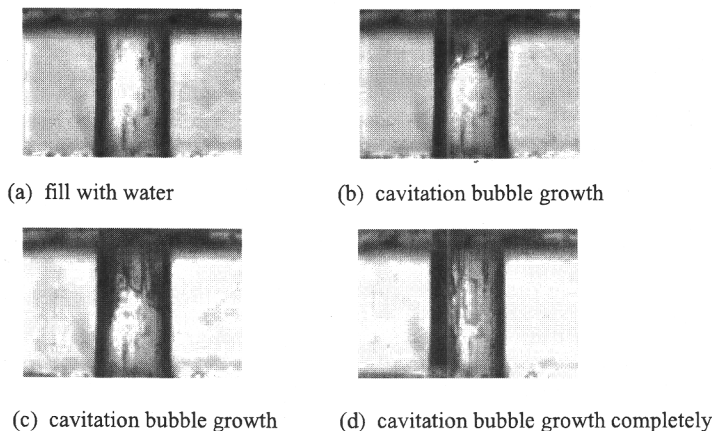


Fig. 7 Image of the liquid flow in the nozzle at the direction of grinding is parallel to the direction of shot corresponding to Fig. 5a: (a) image of the liquid flow in the nozzle with an almost zero velocity; (b,c) image for the cavitation growing condition; (d) image for the cavitation growth completely.

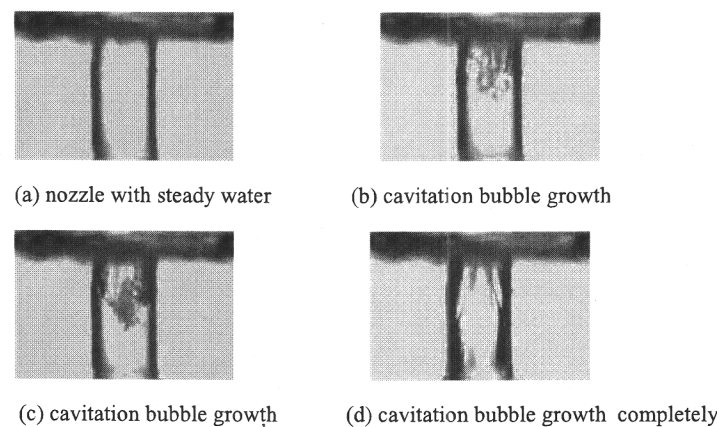


Fig. 8 Image of the liquid flow in the nozzle at the direction of grinding is perpendicular to the direction of shot corresponding to Fig. 5b: (a) image of the liquid flow in the nozzle with an almost zero velocity; (b,c) image for the cavitation growing condition; (d) the image for the cavitation growth completely.

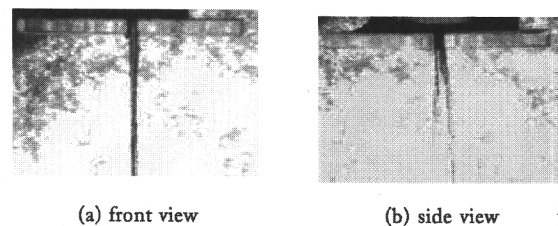


Fig. 9 Photographs of the liquid jet near the exit of the nozzle for the case of $L/D = 2$ ($D = 0.7$ mm); (a) corresponding to Fig. 5a; (b) corresponding to Fig. 5b.

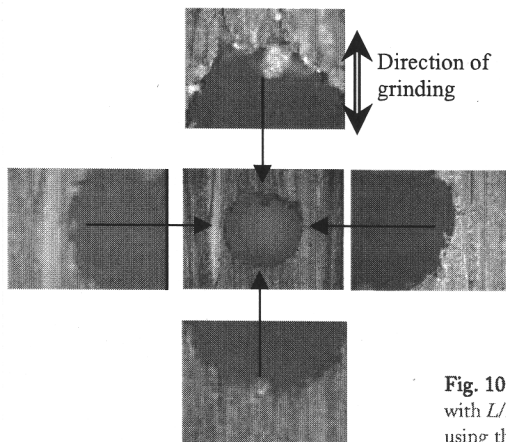
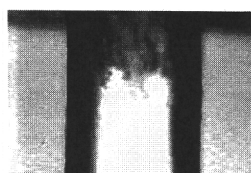


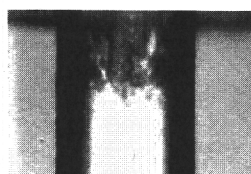
Fig. 10 Top view magnification images of the nozzle hole with $L/D = 2$ ($D = 0.7$ mm) where the orifice was ground by using the grit number 40 sandpaper.

cavitation bubbles is also even in the nozzle hole with $D = 1.5$ mm. Figure 13 shows amplified images of the inlet surface of the nozzle hole with $L/D = 2$ ($D = 1.0$ mm), where the center image is magnified by 50 times and the others images are magnified 200 times; the orifice was ground with grit number 40 sandpaper. Figure 14 is for $D = 1.5$ mm. For comparison with Fig. 9, Figs. 15 and 16 show the exiting liquid jets. It is interesting to note that the shape of the exiting jet appears very circular as the diameter of the nozzle increases. The above results indicate that increasing the diameter of the nozzle hole can reduce the effect of roughness on cavitation and the occurrence of hydraulic flip.

From these quantitative results, the very interesting conclusions are that the characterization of the inhomogeneous occurrence of cavitation exists; the nonappearance of hydraulic flip must be a function of the roughness-to-hole diameter ratio; and the critical value is 0.0115 for the acrylic-water case can be derived.

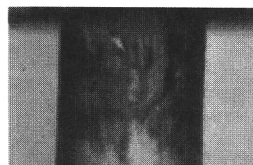


(a)

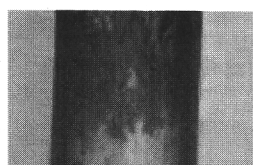


(b)

Fig. 11 Photographs of the liquid flow in the nozzle hole with $L/D = 2$ ($D = 1$ mm): (a) The distribution of cavitation bubbles is even (perpendicular) (corresponding to Fig. 5a); (b) the distribution of cavitation bubbles is even (parallel) (corresponding to Fig. 5b).



(a)



(b)

Fig. 12 Photographs of the liquid flow in the nozzle hole with $L/D = 2$ ($D = 1.5$ mm): (a) The distribution of cavitation bubbles is even (perpendicular) (corresponding to Fig. 5a); (b) the distribution of cavitation bubbles is even (parallel) (corresponding to Fig. 5b).

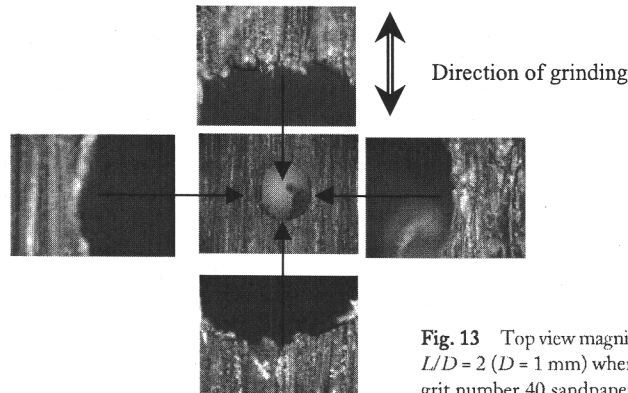


Fig. 13 Top view magnification images of the nozzle hole with $L/D = 2$ ($D = 1$ mm) where the orifice was ground by using the grit number 40 sandpaper.

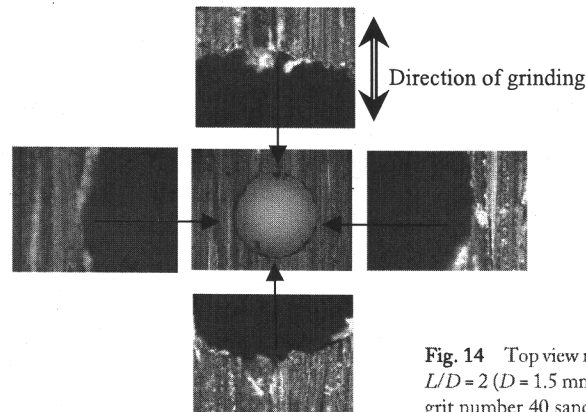


Fig. 14 Top view magnification images of the nozzle hole with $L/D = 2$ ($D = 1.5$ mm) where the orifice was ground by using the grit number 40 sandpaper.

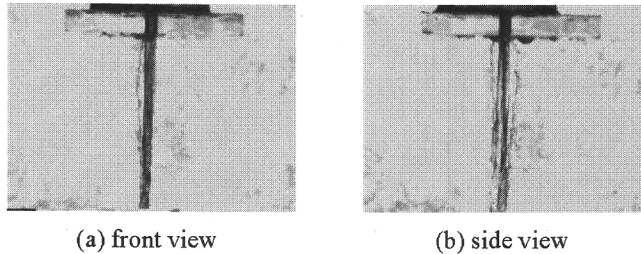


Fig. 15 Photographs of the liquid jet near the exit of the nozzle for the case of $L/D = 2$ ($D = 1$ mm): (a) corresponding to Fig. 5a; (b) corresponding to Fig. 5b.

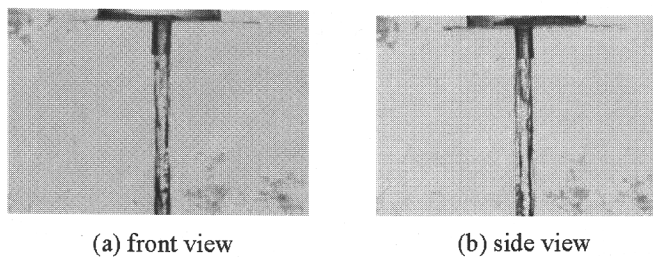


Fig. 16 Photographs of the liquid jet near the exit of the nozzle for the case of $L/D = 2$ ($D = 1.5$ mm): (a) corresponding to Fig. 5a; (b) corresponding to Fig. 5b.

EFFECT OF NOZZLE MATERIAL ON CAVITATION

To investigate the effect of nozzle material on cavitation, four additional materials were used to fabricate four different nozzles (stainless steel, aluminium, copper, and polycarbonate), rather than using different working fluids. The inlet surfaces of the nozzles were ground in the same way as before, but the sandpaper grinding is without orientation, deliberately creating almost the same degree of roughness. According to Dagnall [20], the surface roughness ranges from 1.6 to 6.3 μm when it is fabricated by drilling. A surface roughness of 2.4 μm was chosen for the experiment. Table 3 lists the roughness of the inlet surface for the four nozzles where the values of surface roughness are $\sim 2.4 \mu\text{m}$. Figures 17–20 show the behavior of the liquid jet near the exit of the nozzle with $L/D = 2$ ($D = 0.5$ mm, roughness/hole diameter is 0.0050) for different materials. Table 4 lists the injecting

Table 3 Roughness of Inlet Surface in the Nozzle for the Case with Homogenous Surface Roughness Where the Sandpaper Grinding Is in the Way Without Orientation

Material	Stainless Steel	Copper	Aluminium	Polycarbonate
Roughness (μm)	2.485	2.458	2.409	2.433

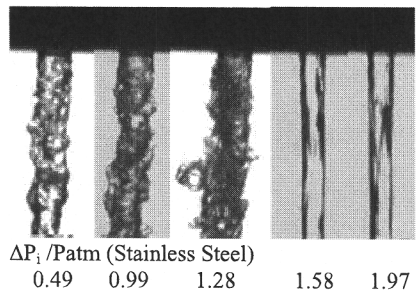


Fig. 17 Behavior of the liquid jet near the exit of the stainless steel nozzle with $L/D = 2$ ($D = 0.5$ mm) where the roughness of nozzle inlet surface is $2.485 \mu\text{m}$.

pressure (dimensionless) when cavitation or hydraulic flip occurs at a surface roughness of $\sim 2.4 \mu\text{m}$ in the four nozzles composed of different materials. It is interesting to note that the phenomena of hydraulic flip jet does not occur with copper and aluminum nozzles, but can be seen only in the stainless-steel nozzle. The results using the stainless-steel nozzle are similar to those of an acrylic nozzle when cavitation occurs during dimensionless driving pressure of 1.28. Hydraulic flip occurs with dimensionless driving pressure of 1.48, using 180 grit-numbered sandpaper, which results in a surface roughness of $3.3 \mu\text{m}$ and roughness-to-hole diameter of 0.0047.

It is worthwhile to mention again that even though the ratios of the roughness and hole diameter in copper, aluminum, and polycarbonate nozzles are 0.0049, 0.0048, 0.0049, respectively (all smaller than 0.0115), the phenomena of hydraulic flip jet cannot be observed in the experiment. Therefore, it is important to investigate this fact and to examine the contact angles of water dropping on the flat surfaces of the various materials, as shown in Fig. 21. The schematic drawing of the contact angle θ is shown in Fig. 22, and listed in Table 5, are considered. The attractive force between water molecules and nozzle material molecules (referred as to "adhesive force"), is affected by the surface roughness of the material in the experiment, which is consistent with the description of Munson et al. [21]. Therefore, the measurements of contact angle are based on the case in which the surface of the material is uniformly ground by sandpaper to make sure that the roughness is homogeneous. The contact angle of the water on the material surface was measured on both the right and left sides to be certain that the surface roughness was homogeneous. To eliminate possible error, 25 measurements were carried out for one case and the mean value

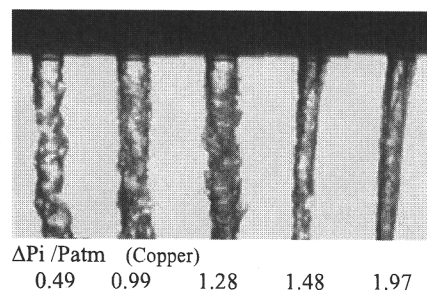


Fig. 18 Behavior of the liquid jet near the exit of the copper nozzle with $L/D = 2$ ($D = 0.5$ mm) where the roughness of nozzle inlet surface is $2.458 \mu\text{m}$.

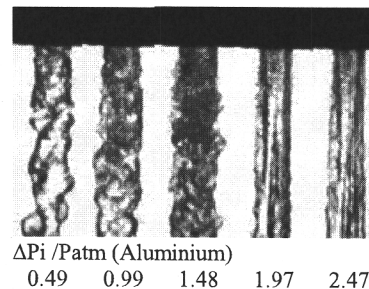


Fig. 19 Behavior of the liquid jet near the exit of the aluminium nozzle with $L/D = 2$ ($D = 0.5$ mm) where the roughness of nozzle inlet surface is $2.409 \mu\text{m}$.

was recorded. The mean value of the contact angle, and of the dimensionless contact angle, the standard deviation of contact angle, and the standard deviation of dimensionless contact angle, are all listed in Table 5. According to Munson et al. [21], in a liquid-gas-solid interface, there is an attraction (adhesion) between the wall of the nozzle and water molecules that is strong enough to overcome the mutual attraction (cohesion) of the water molecules and pull them to the wall. Hence, the water is said to "wet" the wall surface. The angle of $\pi/2$ is used for the nondimension, since the wetting case is referred to the condition of the contact angle $> \pi/2$, and the nonwetting case $< \pi/2$. It should be mentioned that the cavitation cannot be seen since stainless steel, copper, and aluminum are not transparent; therefore there is no V symbol on the table. Also, the values of dimensionless contact angles for copper and aluminium are larger than those of acrylic and stainless steel, which indicates that the adhesion between the wall of the nozzle and the water molecules is greater than the cohesion of water molecules for copper and aluminum nozzles, resulting in the absence of hydraulic flip.

Even though the onset of hydraulic flip in a stainless-steel nozzle with a dimensionless driving pressure of 1.58 is slightly higher than an acrylic nozzle (1.48), it is still consistent with the slightly smaller dimensionless contact angle (1.16) of acrylic (1.19) in relation to the effect of the difference on the roughness-to-hole diameter ratio, where the roughness-to-hole diameter ratio of the steel nozzle is somewhat larger than the acrylic nozzle. Overall, the results indicate that the more adhesion between the wall of the nozzle and water molecules, the lesser the occurrence of hydraulic flip. And there is a critical value for the occurrence of hydraulic flip—between 1.19 and 1.24—when the ratio of the roughness and hole diameter is around 0.0050; however, there is an exception using

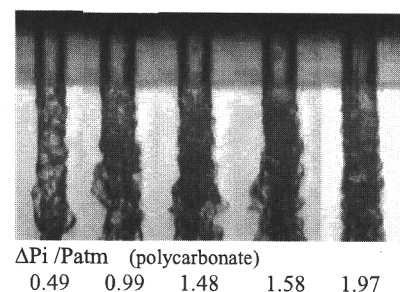


Fig. 20 Behavior of the liquid jet near the exit of the polycarbonate nozzle with $L/D = 2$ ($D = 0.5$ mm) where the roughness of nozzle inlet surface is $2.433 \mu\text{m}$.

Table 4 The Injecting Pressure (Dimensionless) When the Cavitation or Hydraulic Flip Occurs in the Different Material Nozzles Whose Surface Roughness is $\sim 2.4 \mu\text{m}$

Material	$\Delta P_i / \text{Patm}$							
	0.49	0.99	1.28	1.38	1.48	1.58	1.97	2.47
Stainless Steel						O		
Copper								
Aluminium								
Polycarbonate					V			

Note: The length-to-diameter ratio is equal to 2 ($L/D = 2$) and $D = 0.5 \text{ mm}$ ($\text{Patm} = 0.101325 \text{ MPa}$; V: indicates cavitation onset; O: indicates hydraulic flip onset; for stainless steel, copper, and aluminium, the cavitation cannot be seen since the material is not transparent; therefore, there is no V symbol on the table).

polycarbonate, whose contact angle is the smallest (0.82–0.88) in the experiment; but there is no occurrence of hydraulic flip.

It is useful to investigate the surface texture of the polycarbonate plate surface more closely. Figure 23 shows a photograph of polycarbonate surface texture in which the burrs can be seen clearly. According to Chang and Chen [22], the diameter of the burrs can be measured using Metallurgical Microscope and PhotoImpact software for comparison between the burr image and the standard scale, whose dimension was known, and the diameter of burrs ranging from 15 to 30 μm , whose measurement uncertainty is expected to be $\pm 8\%$. It should be mentioned that the burrs are created whenever the material surface is ground with sandpaper. Similarly, burrs will also be created when the nozzle hole is fabricated by drilling. The disappearance of hydraulic flip in the polycarbonate nozzle, which can be seen clearly in Fig. 20., can be attributed to the fact that the burrs on the inside wall of the polycarbonate nozzle can be inserted into the fluid and the flow is interfered whenever the fluid flows in the nozzle in the cavitation condition.

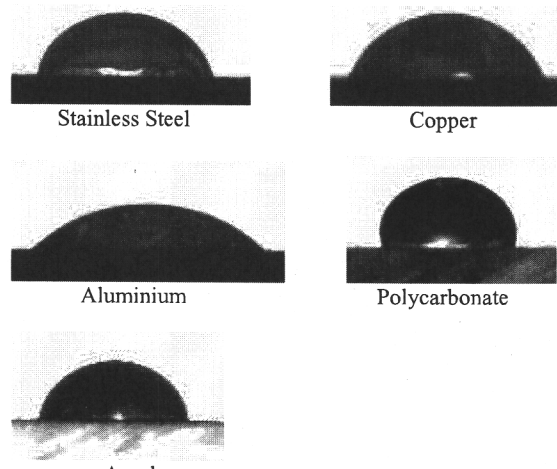
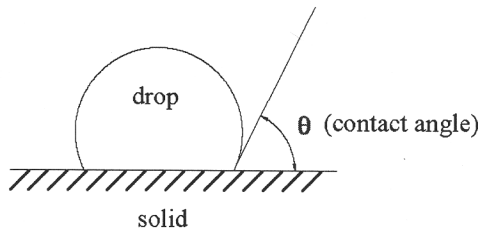


Fig. 21 Contact angles of water drop on the different material surfaces.

Fig. 22 Schematic drawing of the contact angle θ .

CONCLUSIONS

The purpose of this investigation is to clarify the effects of nozzle inlet surfaces with different roughness and sharpness on cavitation or hydraulic flip and to clarify the effect of nozzle material on cavitation. The results are summarized as follows:

The roughness of the nozzle inlet surface does, somewhat, affect the value of the injection pressure at the onset of cavitation and hydraulic flip, respectively. The jet exhibits more surface disturbances in nozzles with rougher inlet surfaces. Moreover, inlet surface roughness can affect the occurrence of cavitation much more than it affects hydraulic flip. The dimensionless driving pressure ranges from 1.28 to 1.48, corresponding to the occurrence of cavitation, and from 1.48 to 1.97, corresponding to the occurrence of hydraulic flip in acrylic nozzles. The variation of dimensionless driving pressure corresponding to the occurrence of cavitation caused by changing surface roughness characterizes a greater extent than hydraulic flip—except when roughness is at $3.29 \mu\text{m}$ and roughness-to-hole diameter ratio is 0.0047.

When the inlet surface is ground to a roughness of $8.05 \mu\text{m}$, where the roughness-to-hole diameter is 0.0115, the phenomenon of hydraulic flip is not obvious and some liquid drops disintegrate from the jet with acrylic/water. Increasing the diameter of nozzle hole can reduce the effect of roughness on the cavitation and reduce the occurrence of hydraulic flip. Overall, characterization of the inhomogeneous occurrence of cavitation and

Table 5 Contact Angle of Water Drop on Different Surface

Material	Polycarbonate		Stainless Steel		Acryl		Copper		Aluminium	
Measurement position	LHS ^a	RHS ^b	LHS	RHS	LHS	RHS	LHS	RHS	LHS	RHS
Mean value of contact angle (degree)	74	79	104	104	107	107	113	112	135	133
Standard deviation of contact angle (degree)	10.02	9.87	9.74	8.27	7.27	5.01	12.14	10.21	8.56	8.79
Mean value of dimensionless of contact angle ($\theta/\text{half of } \pi$)	0.82	0.88	1.16	1.16	1.19	1.19	1.26	1.24	1.50	1.48
Standard deviation of dimensionless of contact angle ($\theta/\text{half of } \pi$)	0.11	0.11	0.11	0.09	0.08	0.06	0.13	0.11	0.10	0.10

^a LHS: 25 measurements taken at the left head side of water drop.^b RHS: 25 measurements taken at the right head side of water drop.

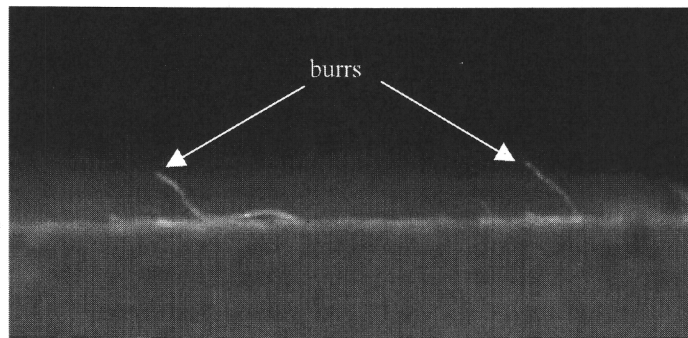


Fig. 23 Photograph of polycarbonate surface texture where the burrs can be seen clearly and its diameter is ranging from about 15 to 30 μm estimated by using the Metallurgical Microscope and PhotoImpact software.

the nonappearance of hydraulic flip must be a function of the ratio of the roughness-to-hole diameter, where the critical value of 0.012 for acrylic/water can be derived.

The more adhesion between the wall of the nozzle and water molecules, the less likely is the occurrence of hydraulic flip, and there is a critical value of the contact angle in dimensionless driving pressure that affects the occurrence of hydraulic flip—between 1.19 and 1.24—when the ratio of the roughness-to-hole diameter is ~ 0.005 . Also, burrs on the inside wall of the nozzle will displace hydraulic flip even though cavitation exists within the nozzle. The disappearance of hydraulic flip in the polycarbonate nozzle can be attributed to the fact that burrs on the inside wall of the nozzle interfere with the flow when they become inserted into the fluid flowing into the nozzle hole. Therefore, cavitation is not only affected by coupling the ratio of the roughness-to-hole diameter and competition for contractive adhesive forces, represented by the contact angle, but it can also be affected by the surface texture inside the nozzle, such as burring. In addition, the results are consistent with previous works that categorize the atomization into two types. One is characterized by short breakup lengths due to the disturbance of liquid flow in the nozzle hole, which is not fully developed in the nozzle passage and results from cavitation. The other atomization is characterized by long breakup lengths caused by cavitation bubbles forming in the sharp inlet corner, fully developing in the nozzle passage, and resulting in hydraulic flip.

REFERENCES

1. W. Bergwerk, Flow Pattern in Diesel Nozzle Spray Holes, *Proc. Inst. Mech. Eng.*, vol. 5, no. 25, pp. 655–660, 1959.
2. H. Hiroyasu, M. Arai, and M. Shimizu, Break-up Length of a Liquid Jet and Internal Flow in a Nozzle, *Proc. ICCLASS-91*, pp. 123–133, 1991.
3. N. Tamaki, M. Shimizu, K. Nishida, and H. Hiroyasu, Effects of Cavitation and Internal Flow on Atomization of a Liquid Jet, *Atomization and Sprays*, vol. 8, pp. 179–197, 1998.
4. H. Hiroyasu, Spray Breakup Mechanism from the Hole-type Nozzle and Its Applications, *Atomization and Sprays*, vol. 10, pp. 511–527, 2000.
5. C. Soterious, R. Andrew, and M. Smith, Direct Injection Diesel Sprays and the Effects of Cavitation and Hydraulic Flip on Atomization, SAE Paper No. 950080, 1995.

6. H. Chaves, M. Knapp, A. Kubitzek, F. Obermeier, and T. Schneider, Experimental Study of Cavitation in the Nozzle Hole of Diesel Injector Using Transparent Nozzles, SAE Paper No. 950290, 1995.
7. M. E. Henry and S. H. Collicott, Visualization of Internal Flow in a Cavitating Slot Orifice, *Atomization and Sprays*, vol. 10, pp. 545–563, 2000.
8. Y. Chen and S. D. Heister, Modeling Cavitating Flows in Diesel Injector, *Atomization and Sprays*, vol. 6, pp. 709–726, 1996.
9. A. H. Lefebvre, *Atomization and Sprays*, Hemisphere, 1989.
10. W. H. Nurick, Orifice Cavitation and Its Effect on Spray Mixing, *J. Fluids Eng.*, pp. 681–687, 1976.
11. D. P. Schmidt and M. L. Corradini, One-Dimensional Analysis of Cavitation Orifices, *8th International Symposium on Transport Phenomena in Combustion*, San Francisco, 1995.
12. D. P. Schmidt, T.-F. Su, K.-H. Goney, P. V. Farrell, and M. L. Corradini, Detection of Cavitation in Fuel Injector Nozzles, *Institute for Liquid Atomization and Spray Systems (ILASS) 9th Annual Conference*, San Francisco, 1996.
13. T. Koivula, On Cavitation in Fluid Power, *Proc. of 1st FPNI-PhD Symp. Hamburg*, pp. 371–382, 2000.
14. K. Nishida, S. Ceccio, D. Assanis, N. Tamaki, and H. Hiroyasu, Characterization of Cavitation Flow in a Simple Hole Nozzle, *Proceedings of ICCLASS-97*, pp. 207–214, 1997.
15. P. M. Gerhart, R. J. Gross, and J. I. Hochstein, *Fundamentals of Fluid Mechanics*, Addison-Wesley, Reading, MA, chap. 1, 1992.
16. F. W. Sears, M. W. Zemansky, and H. D. Young, *College Physics*, Addison-Wesley, Reading, MA, chap. 12, 1980.
17. T. Young, *Miscellaneous Works*, I. G. Peacock, ed., vol. I, Murray, London, p. 418, 1855.
18. C. G. Douglas, *Physics: Principles with Applications*, Prentice-Hall, Englewood Cliffs, NJ, chap. 6, 1984.
19. R. L. David, *Handbook of Chemistry and Physics*, 84th ed., CRC Press, Boca Raton, 2003.
20. H. Dagnall, *Exploring Surface Texture*, Rank Taylor Hobson, Leicester, chap. 1, 1986.
21. B. R. Munson, D. F. Young, and T. H. Okiishi, *Fundamentals of Fluid Mechanics*, 4th ed., chap. 1, Wiley, New York, 2002.
22. J. C. Chang and C. Y. Chen, Experimental Study on Top Venting of Water Solutions with Neutral Polymer of PVP during Emergency Relief, *J. Chin. Soc. Mech. Eng.*, vol. 21, no. 5, pp. 495–503, 2000.